Investigation of the Parameters affecting CO_2 –assisted Polyaniline Polymerization

H. Noby[1,2], A. H. El-Shazly[1], M. F. Elkady[1] and M. Ohshima[3]

[1]*Chemical and Petrochemicals Engineering Department, Egypt-Japan University of Science and Technology, New Borg El-Arab City, Alexandria, Egypt.*
[2]*Material Engineering and Design, Faculty of Energy Engineering, Aswan University, Aswan, Egypt.*
[3]*Chemical Engineering Department, Kyoto University, Kyoto, Japan. 615-8510.*

Abstract. Specific Polyaniline (PANI) morphologies such as nanotubes and nanofiber are required for enhancing its performance in the various applications. CO_2 –assisted Polyaniline polymerization is a method recently used to produce these anticipated morphologies. In this study, polyaniline nanotube was prepared successfully in the presence of compressed CO_2 utilizing Aniline as a monomer and Ammonium peroxydisulfate (APS) as an oxidizing agent. The effect of both reaction temperature and the oxidizing agent feed rate on the morphology and surface area of the produced PANI was investigated. The synthesized PANI was examined by FT-IR, XRD, and BET surface area analysis. Furthermore, SEM was carried out to figure out the morphology of the prepared PANI. It was indicated that Polyaniline nanotubes PANNTs size and homogeneity were affected by the reaction temperature. The averages of the outer and inner diameters of the PANNTs at 25 ^oC, 45 ^oC, 65 ^oC were found to be about (120, 60 nm), (140, 65 nm), and (175, 75 nm) respectively. Also, the produced surface area was slightly augmented with the increase of the temperature. In addition, it was observed that increasing the feeding rate of the APS was associated with the reduction of the size and the surface area of the produced PANI nanotubes.

1. Introduction

The porosity and morphology of Polyaniline (PANI) are the most effective properties that concern its performance [1, 2]. PANI can be easily synthesized in different morphologies as nanofiber, nanoparticles, nanorods, and nanotubes. Besides, Insignificant PANI surface area may restrict the use of PANI powder in many applications, but it may be overcome by manufacturing PANI nanotubes (PANNTs) [3]. Therefore, lately a great attention has been focused on producing PANNTs with and without the aid of templates [1]. Furthermore, many dissimilar techniques, such as template synthesis, interfacial polymerization [4], and self- assembly have been publicized to produce PANNTs [5]. In order to prepare the PANI in advanced morphologies and in a high porous structure, polymerization assisted with subcritical or supercritical CO_2 was used [6-9]. Polymerization of PANI in subcritical and supercritical CO_2 still needs more investigations to demonstrate the influence of different parameters on the produced morphology. In this experimental investigation, PANNTs was prepared by CO2-assisted polymerization. Also, the influence of the reaction temperature and the APS feed rate into the reaction vessel on the attained PANI Morphology and Surface area were acquired.

2. Experimental

2.1 Materials

Aniline, Ammonium peroxydisulfate (APS), Acetic acid, Hydrochloric acid, Ethanol, and Methanol (Wako Pure Chemical Industries, Japan) were used without further purification. Freshly distilled water was used for the preparation of all aqueous solutions and the washing process.

2.2 Polyaniline preparation

The PANNTs were prepared according to the process reported previously [8]. Aniline (0.2 M) solution in 25 ml of distilled water containing 3 ml of acetic acid and 0.25 M of APS solution in another 25 ml of distilled water were prepared. As shown in Fig. 1, the aniline solution was placed in an autoclave (high pressure vessel) connected to a CO_2 pump. Firstly, the autoclave located in an oven to control the reaction temperature. The

temperature varied as 25, 45, 65 ^{o}C to study its effect on the prepared PANI. The CO_2 pressurized into the reactor causing a pressure rise of 9 MPa for 1 hrs. Secondly, APS solution was fed into the vessel by another pump with a constant feeding changed as 0.5, 1, and 1.5 ml/min. Then, the mixture was left to polymerize for 2 hrs. After 2 hrs of polymerization, a valve was opened to release the CO_2 from the main vessel. The prepared polymer was collected, filtered by centrifugation at 5000 rpm for 5 min, and washed by 1 M HCl, Ethanol solutions, and distilled water. Then it was dried at 80 ^{o}C for 24 hrs.

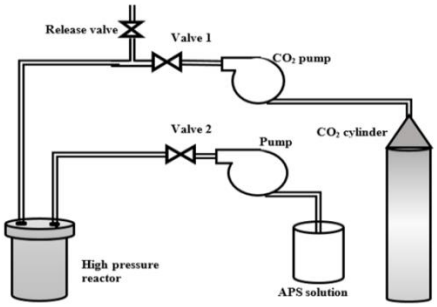

Figure 1. Schematic diagram for the methodology used in PANI CO_2-assisted polymerization.

2.3 Characterization of the prepared PANI

IR spectrometer (Vertex 70, Bruker scientific instruments, Germany) with a wavelength range from 4000 to 400 cm^{-1} was employed to show the FT-IR of the synthesized PANI. The spectrum in the LabX XRD-6100 Shimadzu, Japan, X-ray diffraction was used to show the crystallinity of PANI. N_2 adsorption/desorption isotherms at 77 K and the Brunauer-Emmett Teller (BET) surface area analysis were conducted using (BelsorbminiII, BEl Japan Inc., Japan). All the samples were degassed under vacuum at 150 °C for 2 hrs. Barrett, Joyner and Halenda (BJH) method was employed to determine the pore size distribution and total pore volume. The morphology was observed by scanning electron microscopy SEM (JEOL JSM-6010LV, Japan).

3. Results and discussion

Regarding the improvement of the PANI surface area and attaining advanced PANI morphology, the polymerization temperature and the feed rate of the ABS impact on the manufactured PANI was observed by SEM, BET surface area analysis, XRD, and FT-IR.

3.1 Morphological structure

Fig. 2 shows SEM images of the PANNTs prepared at different temperatures and APS feed rates, where the nanoscale tube-like structure, i.e., Polyaniline Nanotubes (PANNTs) was observed. The effect of temperature on the morphological structure at constant APS flow rate of 0.5 ml/min was determined in Fig. 2 (a, b, and c). Uniform nanotubes of PANI were noticed at low reaction temperature. It was noticed that the uniformity of the nanotubes diminished with the surge of the temperature. Therefore, some nanoparticles were observed at 45 and 65 ^{o}C SEM images.

As seen, a rise of the tubular structure diameter with the increase of temperature was noticed. According to the SEM images, the averages of the outer and inner diameters of the PANNRs at 25 ^{o}C, 45 ^{o}C, 65 ^{o}C were found to be about (120, 60 nm), (140, 65 nm), and (175, 75 nm) respectively. The length of the produced structure was in the range of (1- 2.5 μm). PANI has great thermal stability, so as expected the increasing of the temperature reduces this thermal stability which facilitate the diffusion of the CO_2 molecules into the entire region of PANI before it released. Besides the thermal stability, rising the temperature to 45 or 65 ^{o}C will change the status of the CO_2 from sub-critical to supercritical Sc-CO_2. Sc-CO_2 has better diffusivity into the different solutions compared with the sub-critical; this will resulted in high surface area. Therefore, the BET surface area analysis confirmed this phenomena and showed better surface area with augmentation of the temperature.

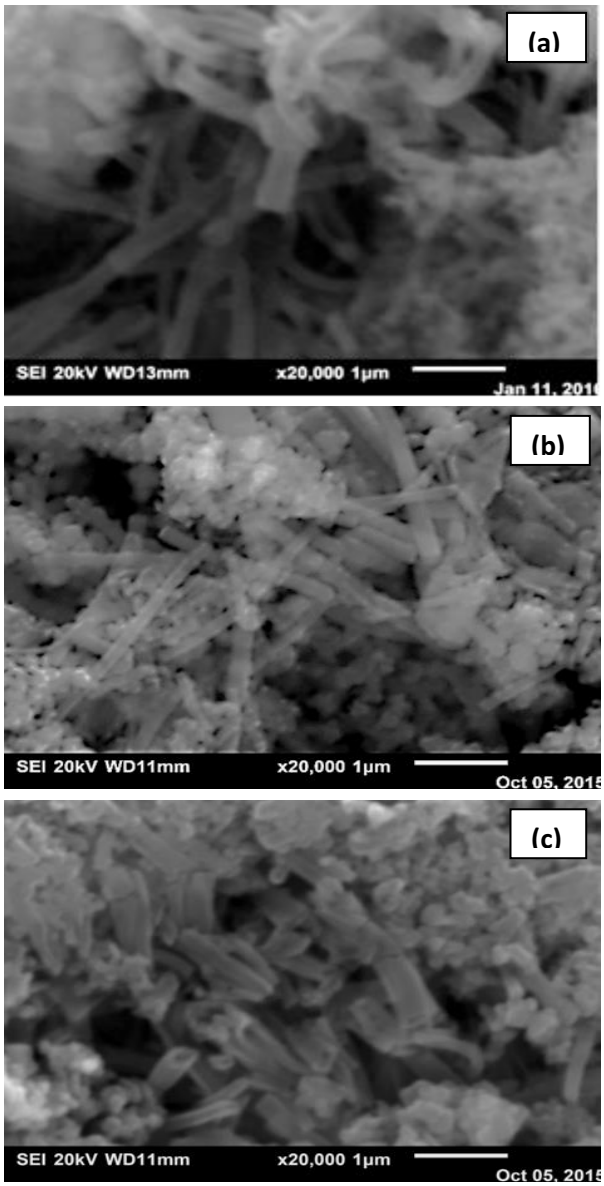

Figure 2. SEM images of the prepared PANNTs with rate of 0.5 ml/min at (a) 25 ^{o}C, (b) 45 ^{o}C, and (c) 65 ^{o}C.

The effect of APS feed rate on the morphological structure was observed in Fig. 2a and 3 (a and b). Almost, uniform nanotubes of PANI were noticed at all APS feed rates. As shown, the rise of the APS feed rate was accompanied by more homogeneous nanotubular structure and diminution of the diameter size. The average outer and inner diameters of the PANNRs at 0.5, 1.5, and 1.5 ml/min were found to be about (160, 75 nm), (140, 65 nm), and (135, 60 nm) respectively. The enlarging of the APS flow rate may increase the contact points between the monomer and the oxidizer which creates more PANI nucleation points. This may cause the lessening of the diameters size.

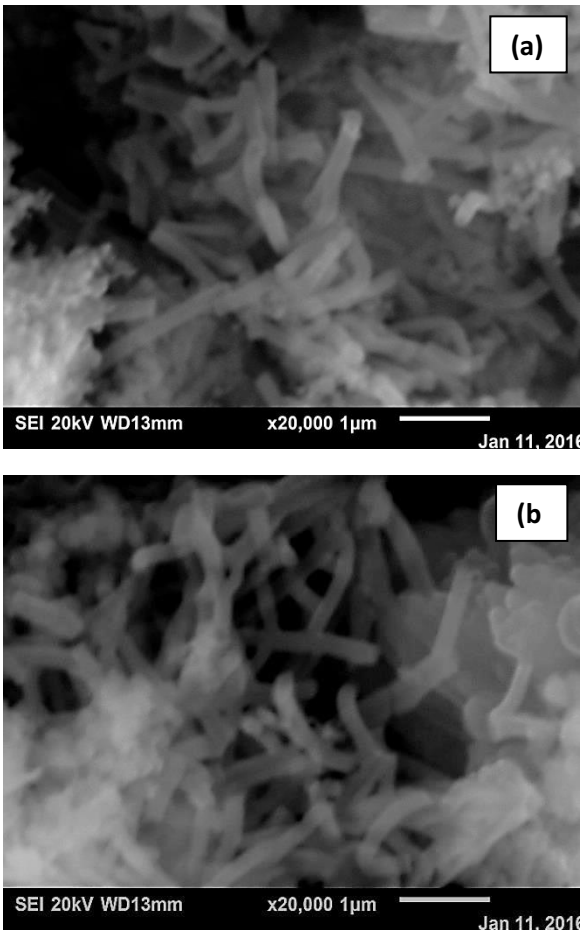

Figure 3. SEM images of the PANNTs prepared at uniform room temperature and (a) 1 ml/min, and (b) 1.5 ml/min.

3.2 Surface area and Pore size

Table 1 shows the BET surface area, the total pore volume and the average pore size of the produced PANNTs different samples. N_2 adsorption/desorption isotherm and pore size distribution of the produced PANI at different reaction temperature were shown in Fig. 4 (a, b, and c). The prepared PANI structures showed a hysteresis loop H3 type according to the IUPAC classification [10]. Also, a wide range pore size distribution (from 1.4 to 70 nm) was observed for all the tested temperatures, which can be considered a macroporous structures according to the IUPAC pores classification. Based on the data of Table 1, the BET surface area of the produced PANNTs samples were 22.13, 25.71, and 28.9 (m^2/g) at 25 °C, 45 °C, 65 °C respectively.

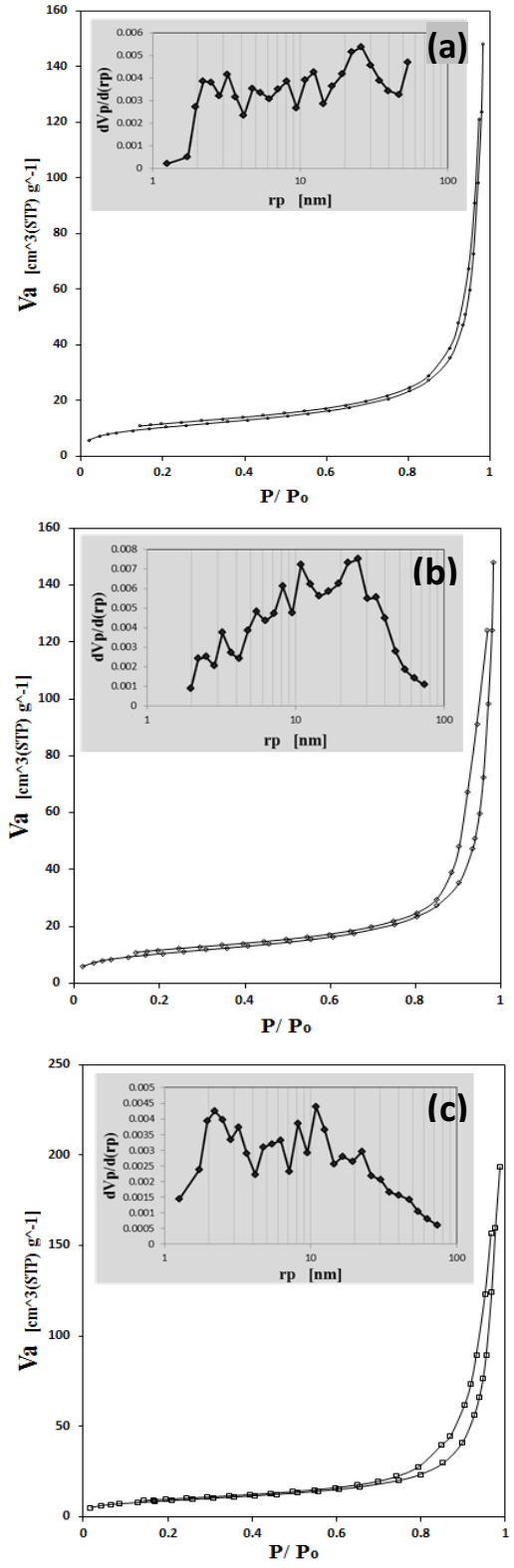

Figure 4. N_2 adsorption-desorption isotherm and pore size distribution of PANNTs with APS feed rate of 0.5 ml/min at (a) 25 °C, (b) 45 °C, and (c) 65 °C.

Fig. 4a and 5 (a, and b) represent the N_2 adsorption/desorption isotherm and pore size distribution of the synthesized PANNTs at various APS feed rates at a

uniform reaction temperature of 25 °C. The hysteresis loop changed from H3 type to H4 with the rise of the feeding rate. This may related to the nanoporous pores attained at the material as confirmed by Table 1. Moreover, the BET surface area of the produced PANNTs samples were diminished until it reached 8.47 (m^2/g) at APS feeding rate of 1.5 ml/min.

Table 1. Surface area, total pore volume, and average pore diameter of different PANI samples.

Parameters	Reaction temperature °C			APS feed rate ml/min		
	25	45	65	0.5	1	1.5
Surface Area (m^2/g)	22.13	25.71	28.9	22.13	18.56	8.47
Total Pore Volume (BJH) (cm^3/g)	0.229	0.286	0.29	0.229	0.187	0.082
Average Pore Size (BJH) (nm)	25.71	27.63	23.6	25.71	24.76	2.5

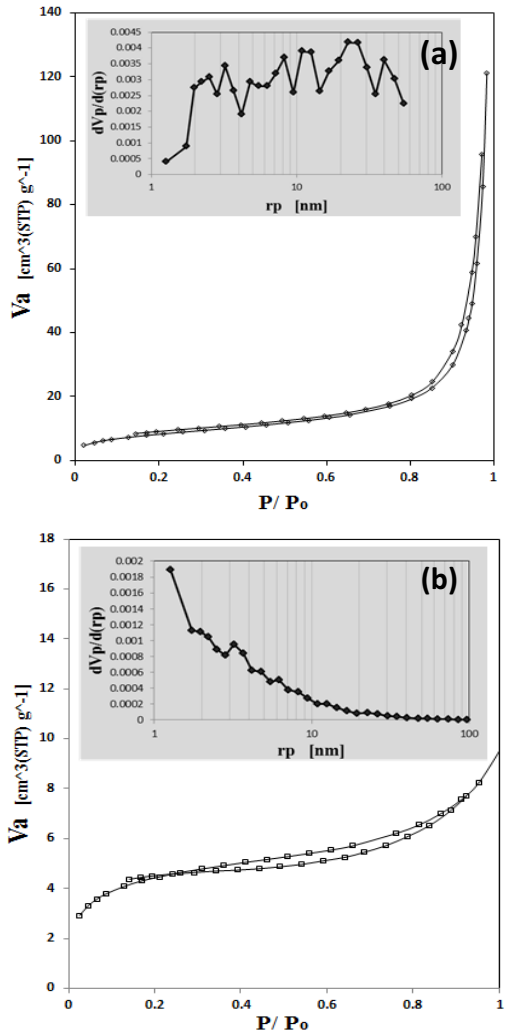

Figure 5. N_2 adsorption-desorption isotherm and pore size distribution of PANNTs at room temperature and (a) 1 ml/min, and (b) 1.5 ml/min.

3.3 Crystalline structure

The crystallinity of the produced PANNTs with different temperatures and feed rates were analyzed by XRD. PANNTs show a characteristic emeraldine salt form. Fig. 6a shows XRD patterns of PANNTs prepared at different temperatures. The XRD pattern of PANI has been reported by several researchers [11-13]. PANI is a semi-crystalline polymer, which has both amorphous and crystals phases. The XRD pattern shows two peaks: one was centered on 2θ=19.38° which attributed to a periodicity parallel to the produced PANI chain and the other was at 2θ=25.7° which associated to a periodicity perpendicular to the polymer chain [12, 13].

XRD patterns of PANNTs prepared at different APS feed rate were figured out in Fig. 6b. Although, no changes were clearly noticed between the XRD peaks of the all attained PANI structure, the crystallinity slightly increased with the rise of the APS feed rate. The high tapered peaks attained with the high feed rate PANI may shows this crystallinity rise.

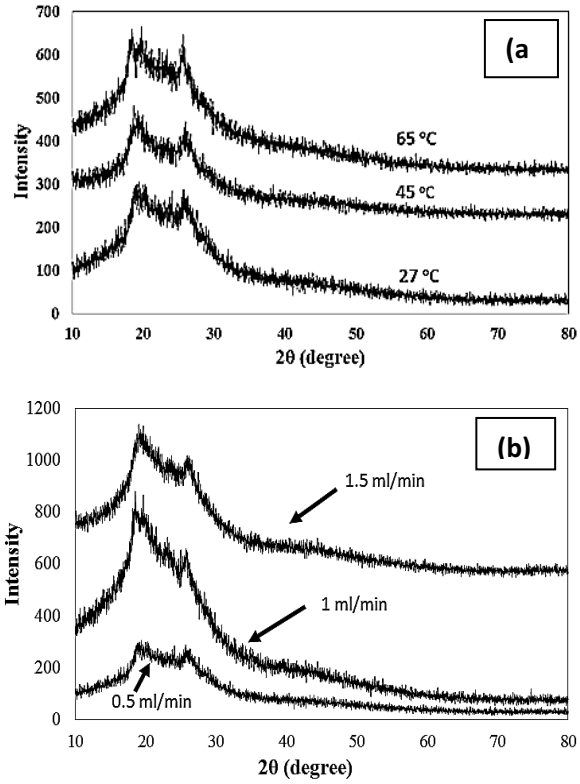

Figure 6. XRD of the prepared PANNTs at (a) different temperatures and uniform feed rate of 0.5 ml/min, (b) different APS feed rates and uniform temperature of 25 °C.

3.4 Chemical structure

The FT-IR of the manufactured PANNTs at various temperatures and APS feed rates were shown in Fig. 7a and 7b. The FT-IR spectra obtained in this study shows the conformity with the previously reported outcomes [11-16]. For all the PANNTs prepared, the characteristic Peaks of the benzenoid and quinoid units performed around 1514 and 1595 cm^{-1} which confirm the existence of the emeraldine salt form due to the approximately

equal benzenoid and quinoid peaks intensity. The peaks at 719 and 1310 cm^{-1} are ascribed to aromatic C—H out-of-plane bending and C—N stretching of the secondary aromatic amine vibrations respectively. The band at 837 cm^{-1} is associated with C—C and C—H for the benzenoid unit. The broad bands in the range of 3000–3500 cm^{-1} are attributed to the free (non-hydrogen bonded) N—H stretching vibration.

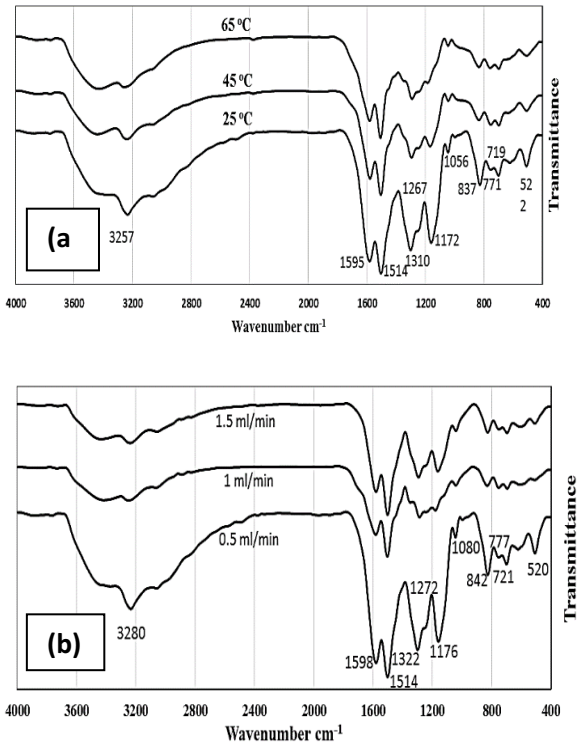

Figure 7. XRD of the all prepared PANNTs at (a) different temperatures at APS feed rate 0.5 ml/min, (b) different APS feed rates at temperature 25 °C.

4. Conclusions

CO_2-assisted polymerization technique was successfully employed to manufacture PANI nanotubes. The main reactants were the Aniline monomer and APS as an oxidizing agent. At first, the compressed CO_2 was diffused into the Aniline solution, and then the APS solution was pumped with a uniform flow rate. The effect of the APS feeding rate and the reaction temperature on the produced PANI morphology and surface area was acquired. According to the SEM, PANNTs size and homogeneity were affected by the reaction temperature variation. The averages of the outer and inner diameters of the PANNRs were assessed to be around (120, 60 nm), (140, 65 nm), and (175, 75 nm) at 25 °C, 45 °C, 65 °C respectively. Moreover, the measured surface area was slightly enlarged with the rise of the temperature. In addition, it was observed that growing the feeding rate of the APS was associated with the reduction of the surface area and size of the synthesized PANI nanotubes.

Acknowledgment

We would like to acknowledge Egypt Japan University for support. We would also like to thank and acknowledge all members of *Materials Process Engineering lab*, *Kyoto University* for their help to conduct the experiment.

References

1. X. Han, H. Qiu, F. Qiu, and J. Yang, Appl. Surf. Sci, (2016).
2. M. Nandi, R. Gangopadhyay, and A. Bhaumik, Microporous Mesoporous Mater., **109**, 239–247, (2008).
3. C. Xu, H. Chen, and F. Jiang, Colloids Surfaces A Physicochem. Eng. Asp., **479**, 60–67, (2015).
4. C. Oueiny, S. Berlioz, and F. X. Perrin, Chem. Phys., **18,** 3504–3509, (2016).
5. Z. Huang, E. Liu, H. Shen, X. Xiang, Y. Tian, C. Xiao, and Z. Mao, Mater. Lett., **65**, 2011, 2018, (2015).
6. Q. Pham, J. Kim, S. Kim, Synth. Met., **160,** 394–399, (2010).
7. J. Du, J. Zhang, B. Han, Z. Liu, and M. Wan, Synth. Met., vol. **155**, 523–526, (2005).
8. H. Noby, A.H. El-Shazly, M.F. Elkady, M. Ohshima, Int. Conf. Chem., Biological and Env. Eng. (ICBEE 2015), (Milan, Italy), 14–15 Sep. (2015).
9. H. Noby, A.H. El-Shazly, M.F. Elkady, M. Ohshima, 13th Int. Conf. Tutorials Adv. Foam Mat. Tech. (FOAMS® 2015), Kyoto, Japan, 10–11 Sep. (2015).
10. K. Kaneko, J. Membrane Sci. **96,** 59-89, (1994).
11. Najim, T.S., Salim, A.J., Arabian J. Chem., (2014), http://dx.doi.org/10.1016/j.arabjc.2014.02.008.
12. L. Ai, J. Jiang, R. Zhang, Syn. Met. **160**, 762–767, (2010).
13. L. Ren, G. Zhang, J. Wang, L. Kang, Z. Lei, Zhongwen L., Z. Liu, Z. Hao, Z. Liu, Electro. Acta **145,** 99–108, (2014).
14. M. Ayad, G. El-Hefnawy, S. Zaghlol, Chem. Eng. J. **217,** 460–465, (2013).
15. J. Wang, K. Zhang, L. Zhao, Chem. Eng. J., **239**, 123–131, (2014).
16. F. Yang, M. Xu, Sh. Bao, H. Wei, H. Chai, Electro. Acta., **137** (2014) 381–387.